

# SPSA ALGORITHM FOR PARACHUTE PARAMETER ESTIMATION

Govindarajan Kothandaraman\*, Mario A. Rotea†  
Purdue University, West Lafayette, IN 47907-1282

This paper presents an algorithm to estimate unknown parameters of parachute models from flight test data. The algorithm is based on the Simultaneous Perturbation Stochastic Approximation (SPSA) method to minimize the prediction error (difference between model output and test data). The algorithm requires only the model output (analytical gradients are not necessary) and it is simple to code. The algorithm is used to estimate aerodynamic and apparent mass coefficients for an existing parachute model.

## Introduction

The contribution of this paper is a simple algorithm for parameter estimation that can be used with nonlinear dynamic parachute models. Model parameters are determined by minimizing the prediction error obtained by comparing model output with test data. Minimization is accomplished using the Simultaneous Perturbation Stochastic Approximation (SPSA) algorithm developed by Spall.<sup>1,2</sup>

The SPSA algorithm is an iterative method for optimization, with randomized search direction, that requires at most three function (model) evaluations at each iteration. Hence, execution time per iteration does not increase with the number of parameters. The method can handle nonlinear dynamic models, non-equilibrium transient test conditions, and data obtained in closed loop. For this reason, this method is suitable for the estimation of parameters in guided parachute models.

The present paper has three main sections. The first section describes the model whose parameters are to be determined. The model is for a G-12 parachute and it was developed at the Naval Post-graduate School (NPS).<sup>3,4</sup> The second section explains the basic parameter estimation approach. This section includes a simple description of the SPSA algorithm. In section three we give the numerical results corresponding to the determination of three aerodynamic coefficients, four apparent mass coefficients, and the initial states for the G-12 parachute model. Conclusions and recommendations for further work are the end of the paper.

## Parachute Model

A six degrees of freedom (6DOF) model of a fully deployed G-12 parachute was developed at NPS.<sup>3,4</sup> Figure 1 gives a schematic of the G-12 parachute. This model assumes the following:

\*Graduate Student, School of Aeronautics and Astronautics.

†Professor, School of Aeronautics and Astronautics, e-mail: rotea@purdue.edu, Corresponding author, Member AIAA

1. The parachute canopy and payload form one rigid system.
2. The aerodynamic forces and moments of the payload are negligible.
3. The aerodynamic forces act at the center of pressure of the canopy, which is nothing but the centroid of the air in the canopy.
4. The G-12 system is symmetrical about the axis joining the canopy centroid to the payload centroid.
5. The parachute is fully deployed.

## Equations of Motion

Let  $m$  be the total mass of the parachute system. Let  $u$ ,  $v$  and  $w$  be the components of the ground velocity of the parachute in the body coordinate system (see Figs. 1 and 2). Let  $p$ ,  $q$  and  $r$  be the components of the angular velocity of the parachute expressed in body coordinates. Then, the equations of motion of the parachute are as follows:<sup>3</sup>

$$\begin{aligned} F_x &= (m + A_{11})(\dot{u} - vr) + (m + A_{33})qw + \\ &\quad (J_1 + A_{15})(\dot{q} + rp) \end{aligned} \quad (1a)$$

$$\begin{aligned} F_y &= (m + A_{11})(\dot{v} + ur) - (m + A_{33})pw - \\ &\quad (J_1 + A_{15})(\dot{p} - qr) \end{aligned} \quad (1b)$$

$$\begin{aligned} F_z &= (m + A_{33})\dot{w} - (m + A_{11})(uq - vp) - \\ &\quad (J_1 + A_{15})(p^2 + q^2) \end{aligned} \quad (1c)$$

$$\begin{aligned} M_x &= (I_{xx} + A_{55})\dot{p} - (J_1 + A_{15})(\dot{v} - pw + ur) - \\ &\quad (I_{yy} + A_{55} - I_{zz})qr + (A_{33} - A_{11})vw \end{aligned} \quad (2a)$$

$$\begin{aligned} M_y &= (I_{yy} + A_{55})\dot{q} + (J_1 + A_{15})(\dot{u} + qw - rv) + \\ &\quad (I_{xx} + A_{55} - I_{zz})pr - (A_{33} - A_{11})uw \end{aligned} \quad (2b)$$

$$M_z = I_{zz}\dot{r} + (I_{yy} - I_{xx})pq \quad (2c)$$

where

$$J_1 = \sum_{i=1}^n m_i z_i \quad (3)$$

$$\sum_{i=1}^n m_i = m \quad (4)$$

and  $z_i$  is the location of the mass center of each of the component masses  $m_i$  of the parachute system. The terms  $A_{11}$ ,  $A_{33}$ ,  $A_{15}$  and  $A_{55}$  are the “apparent mass” terms and are added to account for the acceleration of the fluid around the body. These terms are significant in the case of parachutes because the mass of the parachute is comparable to the mass of the air displaced by it (unlike aircrafts). Expressions for the apparent mass terms were taken from Doherr and Saliaris<sup>5</sup> and are given by

$$A_{11} = \frac{\pi}{3} \rho R_p^3 \quad (5a)$$

$$A_{15} = 0.2 A_{11} \sqrt{R_p^2 + \ell_{SL}^2} \quad (5b)$$

$$A_{33} = 2 A_{11} \quad (5c)$$

$$A_{55} = 0.192 R_p^2 A_{11} \quad (5d)$$

where  $R_p$  is the radius of the inflated canopy and  $\ell_{SL}$  is the length of the suspension lines projected onto the symmetry axis.

The following kinematic equations are used to determine the attitude of the parachute:

$$\dot{\phi} = p + q \sin \phi \tan \theta + r \cos \phi \tan \theta \quad (6a)$$

$$\dot{\theta} = q \cos \phi - r \sin \phi \quad (6b)$$

$$\dot{\psi} = q \sec \theta \sin \phi + r \sec \theta \cos \phi \quad (6c)$$

Finally, the inertial position of the origin of the body coordinates are obtained by integrating Eqn. 7:

$$\begin{aligned} \dot{X} &= u \cos \psi \cos \theta + v (\cos \psi \sin \theta \sin \phi - \sin \psi \cos \phi) \\ &\quad + w (\cos \psi \sin \theta \cos \phi + \sin \psi \sin \phi) \end{aligned} \quad (7a)$$

$$\begin{aligned} \dot{Y} &= u \sin \psi \cos \theta + v (\sin \psi \sin \theta \sin \phi + \cos \psi \cos \phi) \\ &\quad + w (\sin \psi \sin \theta \cos \phi - \cos \psi \sin \phi) \end{aligned} \quad (7b)$$

$$\dot{Z} = -u \sin \theta + v \cos \theta \sin \phi + w \cos \theta \cos \phi \quad (7c)$$

Thus the twelve states can be determined using Eqns. 1–2 and 6–7. See the thesis of Junge<sup>3</sup> for further details.

### Forces and Moments

Before the expressions for the forces and moments are given, certain definitions will be useful. The velocity of the parachute relative to the air (airspeed) is denoted by  $\vec{V}_{air}$  and has components  $u_{air}$ ,  $v_{air}$  and  $w_{air}$  in the body coordinates given by

$$\begin{Bmatrix} u_{air} \\ v_{air} \\ w_{air} \end{Bmatrix} = \begin{Bmatrix} u \\ v \\ w \end{Bmatrix} - \begin{Bmatrix} u_{wind} \\ v_{wind} \\ w_{wind} \end{Bmatrix} \quad (8)$$

where  $u_{wind}$ ,  $v_{wind}$  and  $w_{wind}$  are the components of the wind velocity in body coordinates.

Figure 3 gives the various flight angles used in the determination of force and moment coefficients. Note

that the  $x$ ,  $y$  and  $z$  coordinates shown are the body coordinates.

The total angle of attack is defined by (see Fig. 3)

$$\alpha_T = \arccos \left( \frac{w_{air}}{\sqrt{u_{air}^2 + v_{air}^2 + w_{air}^2}} \right) \quad (9)$$

The angle of attack is given by

$$\alpha = \arctan \left( \frac{u_{air}}{w_{air}} \right) \quad (10)$$

The sideslip angle is given by

$$\beta = \arctan \left( \frac{v_{air}}{\sqrt{u_{air}^2 + w_{air}^2}} \right) \quad (11)$$

The net force on the G-12 parachute is due to the aerodynamic force and gravity. The aerodynamic force  $\vec{F}^{aero}$  is assumed to act at the centroid of the canopy, and has components  $F_x^{aero}$ ,  $F_y^{aero}$  and  $F_z^{aero}$  along the body axes. These components are given by the following relation:

$$\begin{Bmatrix} F_x^{aero} \\ F_y^{aero} \\ F_z^{aero} \end{Bmatrix} = \frac{1}{2} \rho \left( \sqrt{u_{air}^2 + v_{air}^2 + w_{air}^2} \right) \times S_{ref} C_d(\alpha_T) \begin{Bmatrix} u_{air} \\ v_{air} \\ w_{air} \end{Bmatrix} \quad (12)$$

The density of air,  $\rho$ , is a function of the altitude and a standard atmospheric model was used (see Fig. 4).

The drag coefficient  $C_d$  depends on the total angle of attack  $\alpha_T$  and it is shown in Fig. 5. This curve was obtained from the computations of Mosseev.<sup>6</sup>

The gravitational force,  $\vec{F}^{grav}$ , acts along the inertial  $Z$  direction and has the components  $F_x^{grav}$ ,  $F_y^{grav}$  and  $F_z^{grav}$  in body coordinates given by

$$\begin{Bmatrix} F_x^{grav} \\ F_y^{grav} \\ F_z^{grav} \end{Bmatrix} = \begin{Bmatrix} -\sin \theta \\ \cos \theta \sin \phi \\ \cos \theta \cos \phi \end{Bmatrix} mg \quad (13)$$

The net force in the left hand side of Eqn. 1 is the sum of forces in Eqns. 12 and 13.

The moments on the parachute are caused due to the forces described earlier as well as the aerodynamic moments. The aerodynamic moment,  $\vec{M}^{aero}$  has components  $M_x^{aero}$ ,  $M_y^{aero}$  and  $M_z^{aero}$  in the body coordinates given by

$$\begin{Bmatrix} M_x^{aero} \\ M_y^{aero} \\ M_z^{aero} \end{Bmatrix} = \frac{1}{2} \rho (u_{air}^2 + v_{air}^2 + w_{air}^2) \times S_{ref} c_{ref} \begin{Bmatrix} C_m(\beta) \\ C_m(\alpha) \\ 0 \end{Bmatrix} \quad (14)$$

where the variation of  $C_m$  with angle of attack ( $\alpha$ ) or sideslip ( $\beta$ ) is given in Fig. 6. This variation was also obtained from the computations of Mosseev.<sup>6</sup>

As mentioned earlier, the moment due to the aerodynamic forces (assumed to act at the canopy centroid, point C) and weight (acting at the mass center, point D) also need to be accounted for in the final moment that is to be applied to the EOMs. This moment, denoted  $\vec{M}^F$  is given by

$$\vec{M}^F = \vec{R}_{CB} \times \vec{F}^{aero} + \vec{R}_{DB} \times \vec{F}^{grav} \quad (15)$$

where the moment arm  $\vec{R}_{CB}$  is the distance between the canopy centroid (point C) and the origin of the body frame (point B), and  $\vec{R}_{DB}$  is the distance between the center of mass (point D) of the system and the origin (see Fig. 1). For more details, the reader is referred to the thesis of Junge.<sup>3</sup>

The objective of this paper is to improve the parachute model using parameter estimation. In the next section, the  $C_d$  and the  $C_m$  curves will be modified and the parameters that modify these curves will be estimated. Also, the apparent mass terms in Eqn. 5 will be modified and parameters modifying these terms will be estimated. Finally, the initial conditions of the states will also be estimated.

## Parameter Estimation

Once the model structure and the test data are known, the next step is to estimate the parameters of the system. This is done by assuming an initial value of the parameters and then optimizing them so as to minimize the error between the measurements and the model predictions. In this work, a code using standard MATLAB commands, implementing the SPSA algorithm<sup>1,7</sup> for constrained optimization was developed.

The model given in the previous section was modified to reduce the model errors. The modifications are as follows. The aerodynamic force term is determined by Eqn. 12, where the value of the drag coefficient is determined using a lookup table corresponding to Fig. 5. Let this function be denoted by  $C_d^*(\cdot)$ . Consider the following modification to the drag coefficient:

$$C_d(\cdot) = \vartheta_1 + \vartheta_2 C_d^*(\cdot) \quad (16)$$

where,  $\vartheta_1$  is an offset and  $\vartheta_2$  is a scale factor which need to be determined to reduce the model error.

Similarly, consider the moment term. The aero moment is given by Eqn. 14, where the value of the moment coefficient is given by Fig. 6. Let this function be denoted by  $C_m^*(\cdot)$ . Consider the following modification to the moment coefficient:

$$C_m(\cdot) = \vartheta_3 C_m^*(\cdot) \quad (17)$$

Note that the physics of the problem does not allow for a nonzero  $C_m$  at zero angle of attack which ex-

plains the absence of an offset term for the moment coefficient.

Scale factors  $\vartheta_4, \vartheta_5, \vartheta_6$  and  $\vartheta_7$  were incorporated in the apparent mass terms in Eqn. 5 as well and this resulted in

$$A_{11} = \vartheta_4 \frac{\pi}{3} \rho R_p^3 \quad (18a)$$

$$A_{15} = 0.2 \vartheta_5 A_{11} \sqrt{R_p^2 + \ell_{SL}^2} \quad (18b)$$

$$A_{33} = 2 \vartheta_6 A_{11} \quad (18c)$$

$$A_{55} = 0.192 \vartheta_7 R_p^2 A_{11} \quad (18d)$$

The initial conditions of the twelve states were also estimated to get a better fit of the data to the model. This gives an additional twelve unknowns,  $\vartheta_8, \dots, \vartheta_{19}$ .

Thus the vector of unknowns  $\vartheta$  is given by

$$\vartheta = \left\{ \underbrace{\vartheta_1, \vartheta_2, \vartheta_3}_{\text{Aerodyn. params}}, \underbrace{\vartheta_4, \dots, \vartheta_7}_{\text{App. mass terms}}, \underbrace{\vartheta_8, \dots, \vartheta_{19}}_{\text{Initial conditions}} \right\}^T \quad (19)$$

## Method of Parameter Estimation

The Prediction Error Method (PEM) was used to estimate the parameters. PEM estimates parameters by minimizing the difference between the experimental data and the model output.

PEM works by minimizing a cost function. There are many cost functions that can be chosen. Let the measured output vector at time instant  $k$  be denoted by  $y(k)$  and let the predicted output vector at time  $k$  using parameters  $\vartheta$  be denoted by  $\hat{y}(k; \vartheta)$ . Define the prediction error as

$$e(k; \vartheta) = y(k) - \hat{y}(k; \vartheta) \quad (20)$$

A popular cost function is the quadratic function given by

$$H(\vartheta) = \sum_{k=1}^N e(k; \vartheta)^T P e(k; \vartheta) \quad (21)$$

where  $N$  is the total number of time samples and  $P$  is a weighting matrix.  $P$  was chosen to be diagonal and the values of the diagonal elements were chosen so that all the components of  $e(k; \vartheta)$  were normalized and nondimensionalized. This was achieved by choosing the diagonal elements to be the inverse of the square of the infinity-norm of the outputs, i.e.,

$$P(i, j) = \begin{cases} 0, & \text{if } i \neq j \\ \frac{1}{\|\hat{y}_i(\vartheta_0)\|_\infty^2}, & \text{if } i = j \end{cases} \quad (22)$$

where  $\hat{y}_i(\vartheta_0)$  is the prediction of the  $i^{\text{th}}$  measurement obtained from the model using the nominal values of the parameter  $\vartheta$ . Once this value of  $P$  is determined, it can be adjusted to give different weights to different output channels.

## Optimization

A vector of optimal parameters  $\hat{\vartheta}$  is obtained by solving the following problem:

$$\begin{aligned} \hat{\vartheta} &= \arg \min_{\vartheta} H(\vartheta) \\ \text{subject to } &\vartheta_1^{min} \leq \vartheta_1 \leq \vartheta_1^{max} \\ &\vartheta_2^{min} \leq \vartheta_2 \leq \vartheta_2^{max} \\ &\vdots \\ &\vartheta_n^{min} \leq \vartheta_n \leq \vartheta_n^{max} \end{aligned} \quad (23)$$

where the cost function  $H(\vartheta)$  is given in Eqn. 21 and  $n$  gives the total number of parameters, in this case  $n = 19$ .

Most conventional tools used for optimization use the gradient and possibly the Hessian information of the cost function to arrive at a local minimum. However these methods are very time consuming if there are many variables to be optimized or if the cost function evaluations are computationally expensive. If the number of parameters increases, the number of function evaluations required to compute the gradient also increases. Moreover, the chance of a solution converging to a local minimum also increases with the number of parameters to be optimized. For the problem at hand, which has 19 parameters, it was found that the gradient based approach was not practical. For this reason, the Simultaneous Perturbation Stochastic Approximation (SPSA) method was used to minimize the cost function.

### Simultaneous Perturbation Stochastic Approximation

The SPSA is a tool for optimization without the use of costly gradient computations. This method is extremely useful in cases where there are many parameters to be optimized. Spall<sup>1,2</sup> describes the SPSA algorithm and gives some examples where this method proves to be very efficient. Spall<sup>8</sup> gives the theoretical and numerical properties of the algorithm and proves its convergence in a stochastic sense. Sadegh<sup>7</sup> and Wang and Spall<sup>9</sup> describe how the SPSA can be used for constrained optimization as well. The rest of this section is devoted to a brief explanation of the SPSA algorithm, which according to Spall<sup>1</sup> has the following feature:

One properly chosen simultaneous random change in all the variables in a problem provides as much information for optimization as a full set of one-at-a-time changes of each variable.

Consider a cost function  $H$  dependent on parameters  $\vartheta$ . The objective is to minimize  $H(\vartheta)$  subject to some constraints on the values of  $\vartheta$ . The SPSA algorithm minimizes the cost function  $H(\vartheta)$  by using an approximation to the gradient, say  $\hat{g}_k(\vartheta)$ . The

subscript  $k$  indicates the iteration number. The approximate gradient is computed using a properly chosen perturbation vector  $\Delta_k$  which is used in a central difference scheme around the current value of the variables  $\hat{\vartheta}_k$ . Since a central difference scheme is used, two cost function evaluations are required per iterations to compute the approximation to the gradient. Once the approximate gradient is computed the parameters are updated and a new value of  $\vartheta$  is computed. Spall<sup>1</sup> recommends one more cost function evaluation at this point to check if the cost function at this new value of  $\vartheta$  is less than the cost function using  $\hat{\vartheta}_k$ . Thus there are three cost function computations at each iteration. The number of cost function evaluations per iteration *does not* depend on the number of variables, which makes this method very attractive for optimization problems with several variables. However, the drawback of this method is that there are several parameters in the algorithm that have to be tuned. These will be clear when the algorithm is explained later. However, Spall<sup>1</sup> gives guidelines on how to choose initial values for these parameters.

The basic algorithm<sup>1</sup> is as follows:

1. *Initialization and coefficient selection.* Set counter index  $k = 1$ . Pick initial guess for  $\vartheta$  and non-negative coefficients  $a, c, A, \alpha$ , and  $\gamma$  in the SPSA gain sequences  $a_k = a/(A + k)^\alpha$  and  $c_k = c/k^\gamma$ . The choice of gain sequences ( $a_k$  and  $c_k$ ) is critical to the performance of SPSA.
2. *Generation of the simultaneous perturbation vector.* Generate by Monte-Carlo a  $n$ -dimensional random perturbation vector  $\Delta_k$  where each of the  $n$  components of  $\Delta_k$ , i.e.  $\Delta_{ki}$  are independently generated from a zero mean probability distribution with finite inverse moments  $E(|\Delta_{ki}^{-1}|)$  for all  $k, i$ . A simple and theoretically valid choice is to use a Bernoulli  $\pm 1$  distribution with probability  $1/2$  for each  $\pm 1$  outcome. Note that the uniform and normal distributions do not satisfy these conditions. The Bernoulli  $\pm 1$  distribution was used in this paper.
3. *Cost function evaluations.* Obtain two measurements of the cost function  $H(\cdot)$  based on the simultaneous perturbation around the current  $\hat{\vartheta}_k$ :  $H(\hat{\vartheta}_k + c_k \Delta_k)$  and  $H(\hat{\vartheta}_k - c_k \Delta_k)$  with the  $c_k$  and  $\Delta_k$  from Steps 1 and 2.
4. *Gradient approximation.* Generate the simultaneous perturbation approximation to the unknown gradient  $g(\hat{\vartheta}_k)$ . That is,

$$\hat{g}_k(\hat{\vartheta}_k) = \frac{H(\hat{\vartheta}_k + c_k \Delta_k) - H(\hat{\vartheta}_k - c_k \Delta_k)}{2c_k} \begin{bmatrix} \Delta_{k1}^{-1} \\ \Delta_{k2}^{-1} \\ \vdots \\ \Delta_{kp}^{-1} \end{bmatrix},$$

where  $\Delta_{ki}$  is the  $i$ th component of the  $\Delta_k$  vector; note that the common numerator in all the  $p$  components of  $\hat{g}_k(\hat{\vartheta}_k)$  reflects the simultaneous perturbations of all components in  $\hat{\vartheta}_k$  in contrast to the component-by-component perturbations in the standard finite-difference approximation.

5. *Updating  $\vartheta$  estimate.* Use

$$\hat{\vartheta}_{k+1} = \hat{\vartheta}_k - a_k \hat{g}_k(\hat{\vartheta}_k)$$

to update  $\hat{\vartheta}_k$  to a new value  $\hat{\vartheta}_{k+1}$ . If  $\hat{\vartheta}_{k+1}$  falls outside the range of allowable values for  $\vartheta$ , then project the updated  $\hat{\vartheta}_{k+1}$  to the nearest boundary and reassign this projected value as  $\hat{\vartheta}_{k+1}$ . Mathematically we have, for every  $i = 1, \dots, n$ :

$$\hat{\vartheta}_{k+1,i} = \begin{cases} \hat{\vartheta}_{k+1,i} & \text{if } \vartheta_i^{min} \leq \hat{\vartheta}_{k+1,i} \leq \vartheta_i^{max} \\ \vartheta_i^{min} & \text{if } \hat{\vartheta}_{k+1,i} < \vartheta_i^{min} \\ \vartheta_i^{max} & \text{if } \hat{\vartheta}_{k+1,i} > \vartheta_i^{max} \end{cases}$$

Modifications to this step may be needed to enhance the convergence of the algorithm. In particular the update could be blocked if the cost function actually worsens after the “basic” update in this step.

6. *Iteration or termination.* Return to Step 2 with  $k+1$  replacing  $k$ . Terminate the algorithm if there is little change in several iterates or if the maximum number of allowable iterations have been reached.

The choice of various parameters of the algorithm play an important role in the convergence of the algorithm. Spall<sup>2</sup> suggests that  $\alpha = 0.602$  and  $\gamma = 0.101$  are practically effective and theoretically valid choices. Hence these values were used in this paper as well. The value of  $A$  is chosen to be about 10% of the maximum iterations allowed. The maximum number of iterations was chosen to be 100 and hence  $A$  was chosen to be 10. Spall<sup>2</sup> recommends that if the measurements are (almost) error free,  $c$  can be chosen as a small positive number. In this case it was chosen to be 0.01. Spall<sup>2</sup> explains that the value of  $a$  should be chosen such that the  $a/(A + 1)^\alpha$  times the magnitude of elements of  $\hat{g}_0(\hat{\vartheta}_0)$  is approximately equal to the smallest of the desired change magnitudes among the elements of  $\vartheta$  in early iterations. For the problem at hand  $a = 1$  gave good results. This value of  $a$  was chosen to ensure that the components of  $\vartheta$  during the iterations would remain within the allowed bounds, viz.  $\vartheta_{min}^i$  to  $\vartheta_{max}^i$ .

## Results

This section gives the results of parameter estimation where all twelve initial conditions and seven model parameters are determined (see Eqn. 19). These parameters are estimated using SPSA. Forty cases

were run to determine a simple statistics for the estimated parameters. In each case the initial guesses for the aerodynamic and apparent mass parameters  $\vartheta_1, \dots, \vartheta_7$  are different. The initial guesses of the unknown parameters were chosen randomly from a uniform distribution between the maximum and minimum values allowed for these parameters. The following bounds were used for the nondimensional parameters:

$$\begin{aligned} 0.4 &\leq \vartheta_1 \leq 1 & 0 &\leq \vartheta_2 \leq 1.5 \\ 0.5 &\leq \vartheta_3 \leq 2 & 0 &\leq \vartheta_4 \leq 3 \\ 0 &\leq \vartheta_5 \leq 3 & 0 &\leq \vartheta_6 \leq 3 \\ 0 &\leq \vartheta_7 \leq 3 \end{aligned}$$

The wind input used is taken from Junge’s thesis<sup>3</sup> and it is shown in Figs. 7–8. The test data used consists of the inertial positions and velocity shown as the solid lines in Figs. 10–15

After running SPSA forty cases are obtained. Figure 9 shows the histogram of the prediction error (the cost function). Over 80% of the cases attained a cost function value between 5 and 8. Only two cases (the last two bins) have a much higher cost function value, indicating that for these cases SPSA did not converge to a global minimum. Those cases should be removed from further consideration as they are “outliers” that result from a local (and not global) optimization.

Table 1 gives the results of parameter estimation for the aerodynamic and apparent mass parameters,  $\vartheta_1, \dots, \vartheta_7$ . Simple statistics, computed after removing the outliers, are shown for each parameter. The parameter estimation algorithm is successful when it reduces the initial uncertainty in the parameters; i.e., when the standard deviation (STD) is reduced by the algorithm. This is the case with the  $C_d$  offset ( $\vartheta_1$ ) and  $C_d$  scale factor ( $\vartheta_2$ ) where the standard deviation of the SPSA estimates is smaller than that of the initial guesses. On the other hand, the standard deviation of the  $C_m$  coefficient and the apparent mass scale factors did not decrease. This could be because the cost function did not take into account the states corresponding to the rotational motion, viz.  $p, q, r, \phi, \theta$  and  $\psi$  since these measurements were not available. That is, the moment coefficient scale factor and the apparent mass terms do not seem to be identifiable from the available trajectory data.

A single model may now be constructed using the median values of the estimated parameters from Table 1. Figures 10–15 give the measured and simulated position and velocity data of the system using the median parameter values given in Table 1. Figs. 16–17 give the trajectory of the parachute on the  $X - Y$  (ground) plane and in 3D space respectively.

Figures 18–23 give the state estimation errors. The position errors fall within two parachute lengths at all times (one parachute length = 98.46 ft). Finally, Fig. 24 gives the correlation between the input  $X$ -

**Table 1 Results of Parameter Estimation.**

Parameter	Initial Guess			Estimate (using SPSA)		
	Mean	Median	STD	Mean	Median	STD
$C_d$ offset	0.7267	0.6916	0.1795	0.6249	0.6743	0.0893
$C_d$ scale factor	0.5718	0.5293	0.4373	0.0978	0.0270	0.1244
$C_m$ scale factor	1.2745	1.2542	0.4214	1.2702	1.2548	0.4234
$A_{11}$ scale factor	1.5360	1.7042	0.7553	1.5047	1.4718	0.7943
$A_{15}$ scale factor	1.5910	1.6353	0.8996	1.5091	1.4677	0.8690
$A_{33}$ scale factor	1.5833	1.6369	0.6903	1.5871	1.5594	0.7169
$A_{55}$ scale factor	1.6331	1.8531	0.8751	1.6793	1.7241	0.9011

wind (see Fig. 7) and the output error (see Fig. 18). In this figure we observe the correlation between the position error and the input wind velocity. This correlation leads to the conclusion that there is scope for improvement of the present model.

## Conclusions

An algorithm was developed to estimate the parameters of parachute dynamic models. The algorithm is based on the constrained SPSA method, which is capable of optimizing any number of parameters in reasonable time. This is because the number of cost function evaluations needed to estimate the gradient is independent of the number of parameters to be optimized.

The algorithm was applied to the model of a G-12 parachute developed at NPS.<sup>3,4</sup> The match between the estimated and measured position has been good and the error was always less than two parachute lengths. However, it is clear that the parameters associated with rotational motion (e.g.  $C_m$ ) could not be estimated. In principle, this could be due to a lack of measurements of body rates or Euler angles.

The apparent mass coefficients are also not identifiable from the available test data. From the force and moment equations, Eqns. 1 and 2, one may deduce that the apparent mass coefficients would be identifiable only if the accelerations are high enough so that the effect of the apparent mass is visible in the measured states. This was not the case in this particular test.

Future parameter estimation work would require rotational and attitude data to estimate moment coefficient and apparent mass. Also, the uncertainty in apparent mass coefficients would be reduced if the accelerations during the test are high. Test data with relatively large and persistent variations of the angle of attack (total and in longitudinal plane) and side-slip angle would be useful to accurately characterize the variations of the moment and force coefficients with these angles. Finally, future work should make use of refined (controlled) parachute models as recently obtained by Dobrokhodov et al.<sup>4</sup>

## Acknowledgment

The authors are grateful to Rick Howard, Isaac Kaminer, J. Johnson, Christopher Junge, O. Yakinmenko, and V. Dobrokhodov from NPS and to Scott Dellicker from the US Army Yuma Proving Ground for their help with questions about parachute dynamic models and test data. This work was performed with funding from Naval Postgraduate School under contract Nos. N00244-00-P-3258 and N00244-01-P-2540.

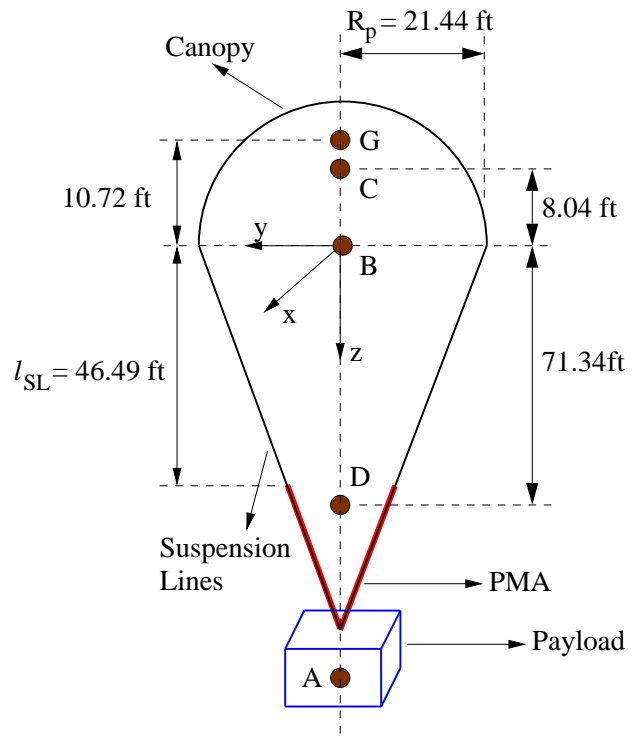


**Fig. 1 G-12 parachute dimensions (not to scale).**

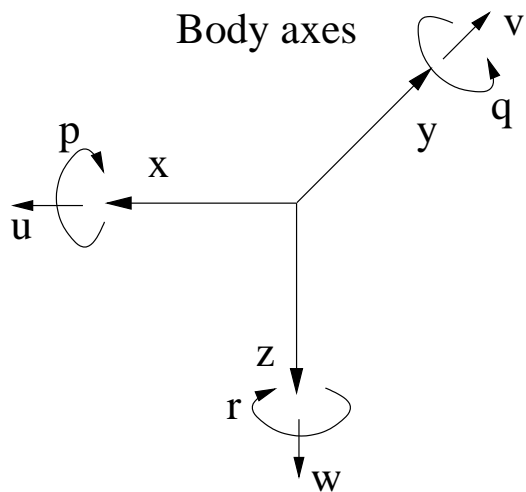


Fig. 2 Body components of angular and ground velocities.

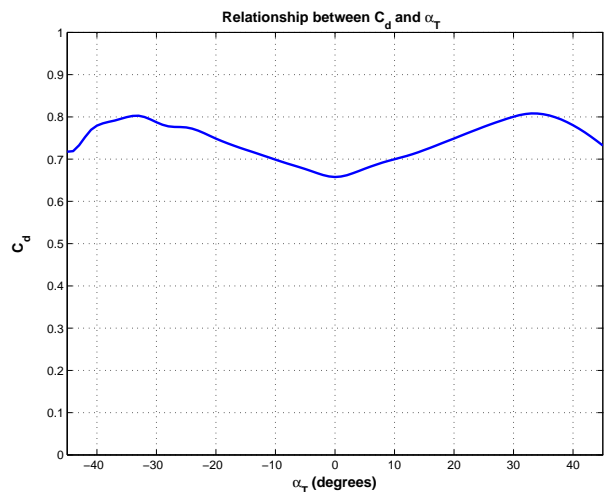


Fig. 5 Drag coefficient data.

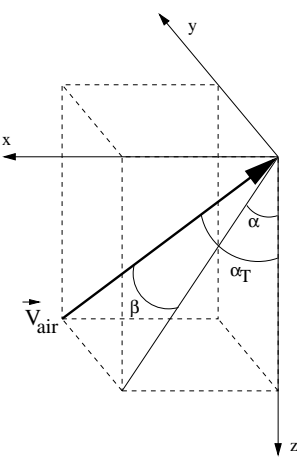


Fig. 3 Flight angles definition.

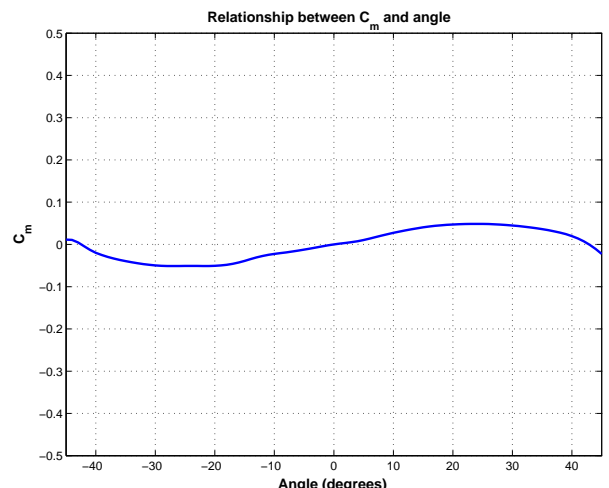


Fig. 6 Moment coefficient data.

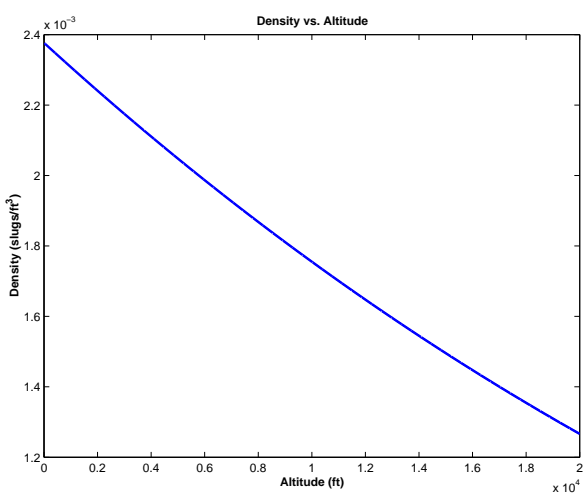


Fig. 4 Density  $\rho$  as a function of altitude.

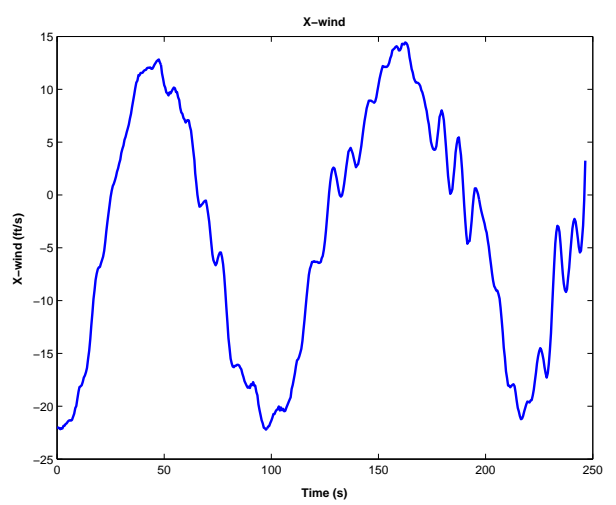
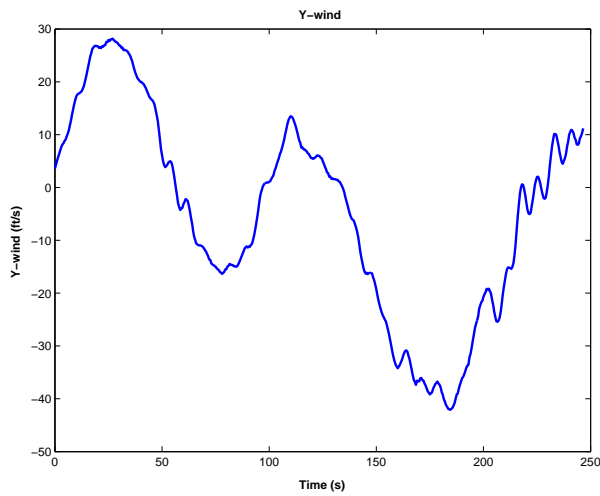
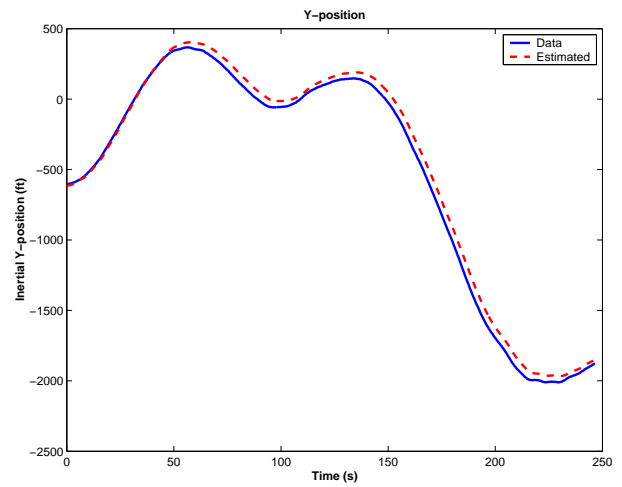


Fig. 7 X-wind.



**Fig. 8 Y-wind.**



**Fig. 11 Y-position.**

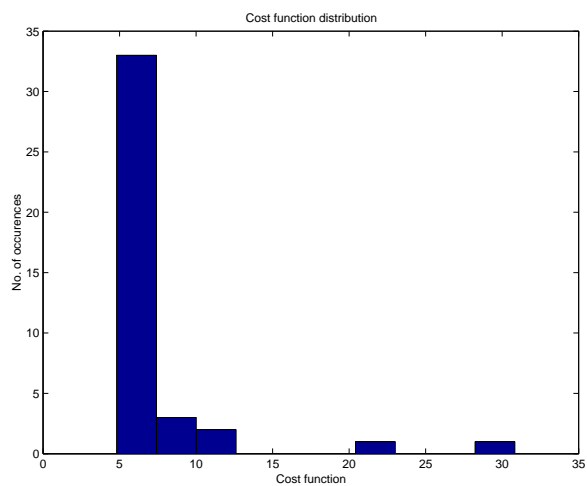


**Fig. 9 Cost function distribution.**

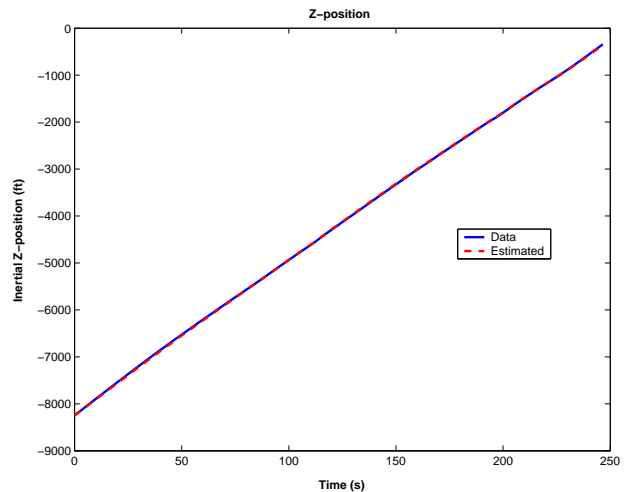


**Fig. 12 Z-position.**

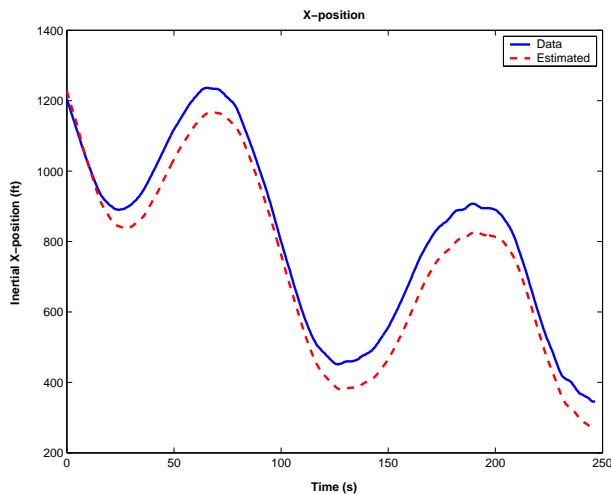


**Fig. 10 X-position.**

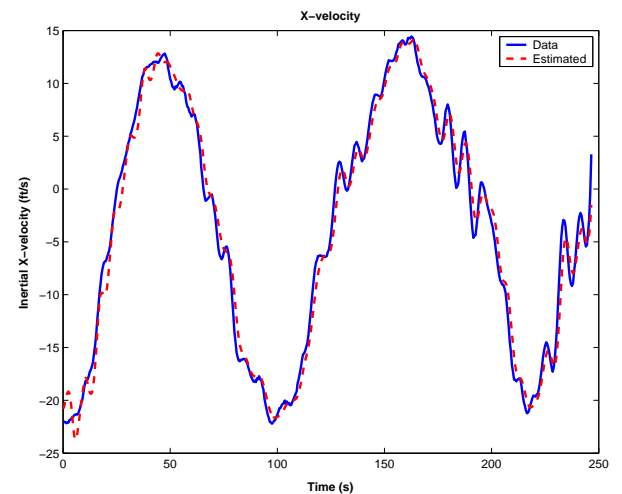


**Fig. 13 X-velocity.**

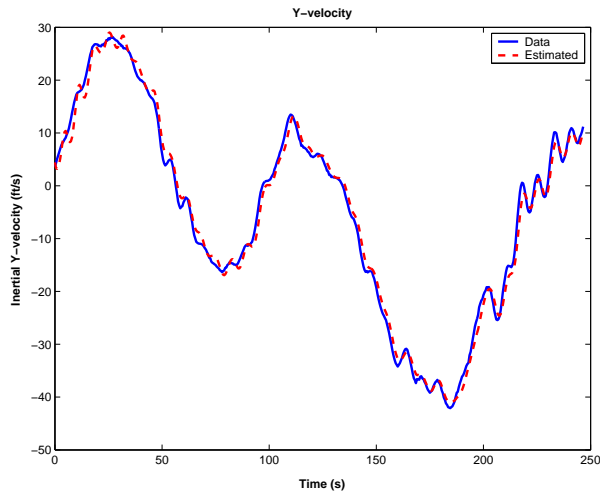


**Fig. 14 Y-velocity.**

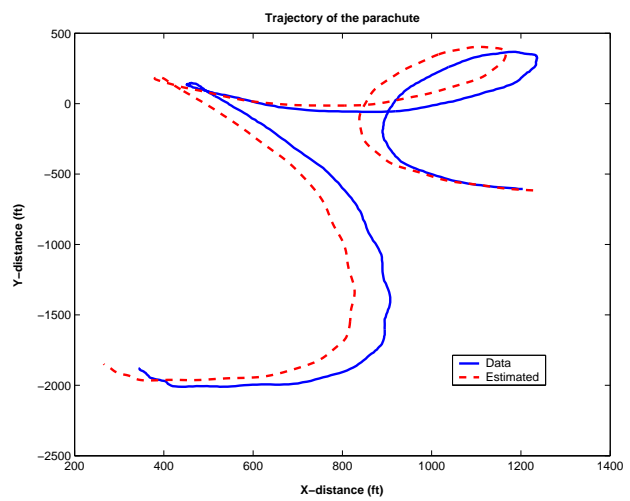


**Fig. 16 Parachute trajectory in the horizontal plane.**

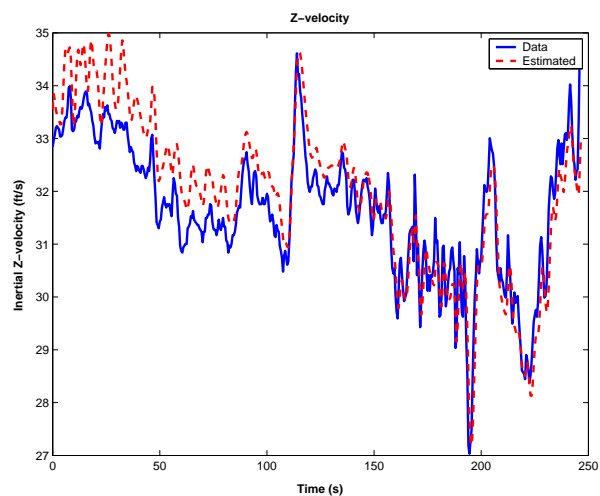


**Fig. 15 Z-velocity.**

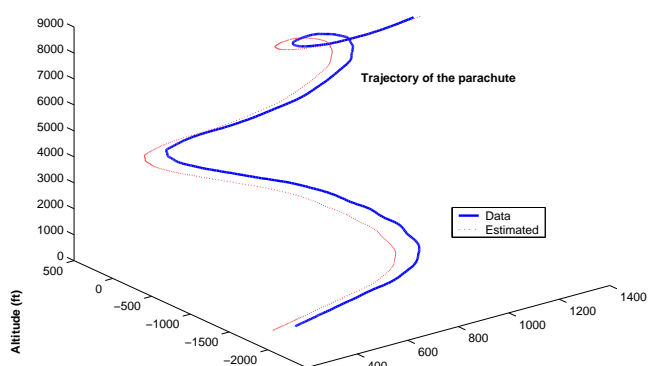


**Fig. 17 Parachute trajectory.**

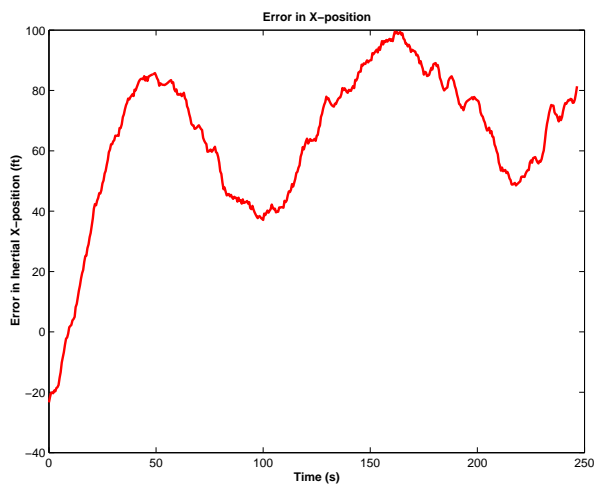


**Fig. 18 Error in X-position.**

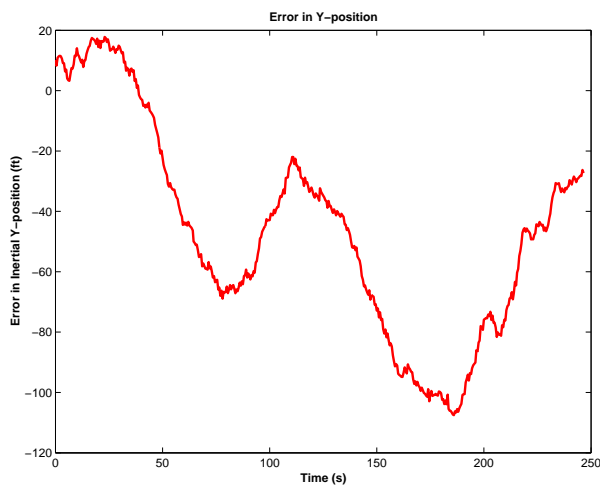


**Fig. 19** Error in Y-position.

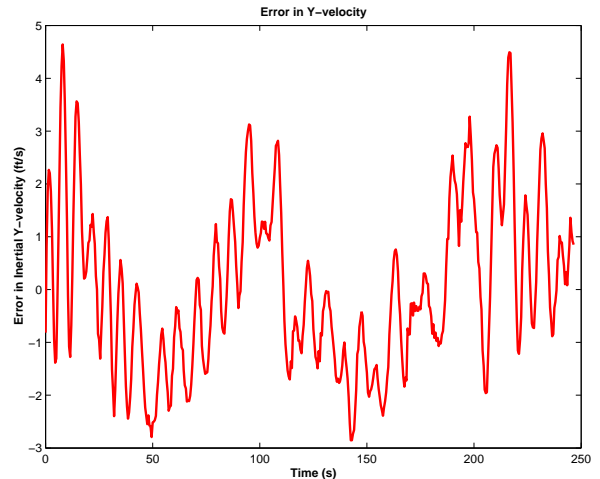


**Fig. 22** Error in Y-velocity.

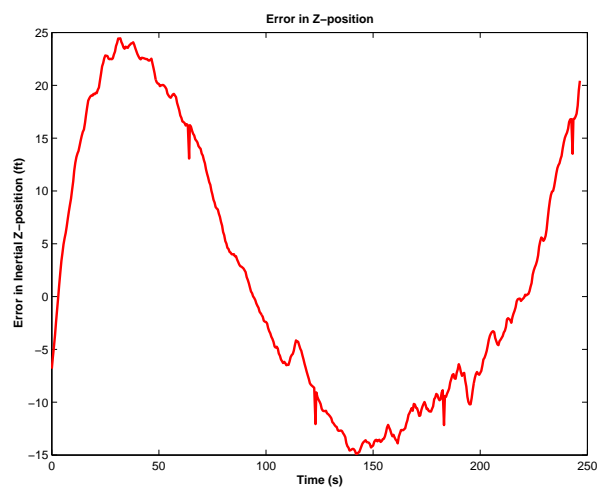


**Fig. 20** Error in Z-position.

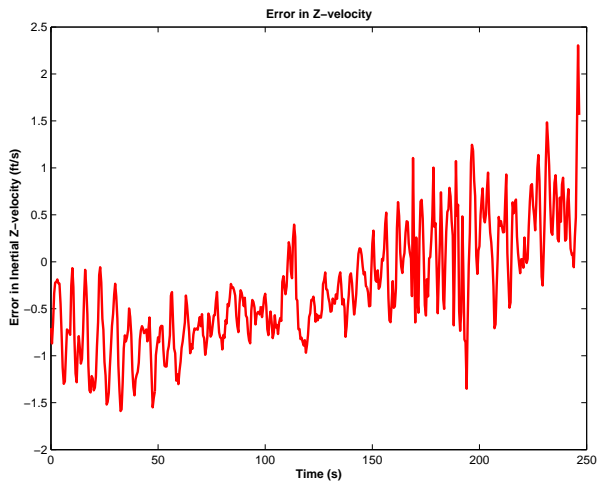


**Fig. 23** Error in Z-velocity.

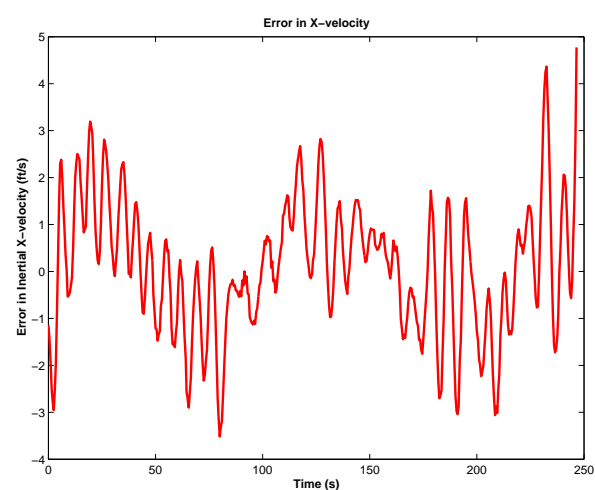


**Fig. 21** Error in X-velocity.

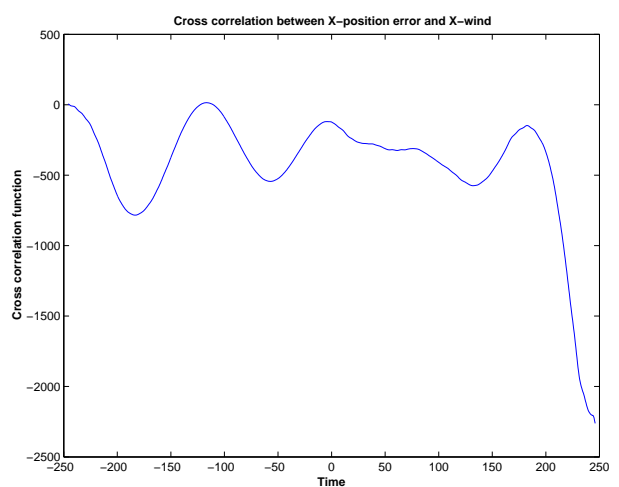


**Fig. 24** Cross correlation between X-wind and X-position error.

## References

<sup>1</sup>Spall, J. C., "An Overview of the Simultaneous Perturbation Method for Efficient Optimization," *John Hopkins APL Technical Digest*, Vol. 19, No. 4, 1998, pp. 482–492.

<sup>2</sup>Spall, J. C., "Implementation of the Simultaneous Perturbation Algorithm for Stochastic Optimization," *IEEE Transactions on Aerospace and Electronic Systems*, Vol. 34, No. 3, July 1998, pp. 817–823.

<sup>3</sup>Junge, C. D., *Development of a Six-Degree-of-Freedom Model for a Fully Deployed G-12 AGAS Delivery System*, Master's thesis, Naval Postgraduate School, Monterey, CA, Dec. 2001.

<sup>4</sup>Dobrokhodov, V., Yakimenko, O., and Junge, C., "Development of a Six-Degree-of-Freedom Model of a Controlled Circular Parachute," Naval Postgraduate School, Monterey, CA. Preprint.

<sup>5</sup>Doherr, K.-F. and Saliaris, C., "On the Influence of Stochastic and Acceleration Dependent Aerodynamic Forces on the Dynamic Stability of Parachutes," *Proceedings of the AIAA 7th Aerodynamic Decelerator and Balloon Technology Conference*, No. AIAA-81-1941, October 1981.

<sup>6</sup>Mosseev, Y., "Fluid Structure Interaction Simulation of the US Army G-12 Parachute," Tech. Rep. 17-01-RDDOzon, Naval Postgraduate School, October 2001, Contract N 68171-01-M-6342.

<sup>7</sup>Sadegh, P., "Constrained Optimization via Stochastic Approximation with a Simultaneous Perturbation Gradient Approximation," *Automatica*, Vol. 33, No. 5, 1997, pp. 889–892.

<sup>8</sup>Spall, J. C., "Multivariate Stochastic Approximation Using a Simultaneous Perturbation Gradient," *IEEE Transactions on Automatic Control*, Vol. 37, No. 3, March 1992, pp. 332–341.

<sup>9</sup>Wang, I.-J. and Spall, J. C., "A Constrained Simultaneous Perturbation Stochastic Approximation Algorithm Based on Penalty Functions," *Proceedings of the American Control Conference*, June 2–4 1999, pp. 393–399.